

PREPARATION AND CHARACTERIZATION OF MANGANESE DOPED ZINC SULPHIDE NANOCRYSTALLINE POWDERS WITH LUMINESCENT PROPERTIES

ADRIAN-IONUȚ CADÎȘ^{a,b}, ADRIAN RAUL TOMȘA^a, ECATERINA BICA^a,
LUCIAN BARBU-TUDORAN^c, LUMINIȚA SILAGHI-DUMITRESCU^b,
ELISABETH-JEANNE POPOVICI^a

ABSTRACT. Manganese-doped zinc sulphide nanocrystalline powders have been synthesized from zinc-manganese acetate and sodium sulphide, in aqueous solution containing methacrylic acid. Precipitation was performed at low temperature, using the sequential reagent addition technique. Different Mn^{2+} concentrations have been used to control the optical properties of ZnS:Mn^{2+} nanoparticles. All samples were characterized by thermal analysis (TGA), infrared absorption spectroscopy (FT-IR), photoluminescence spectroscopy (PL), scanning (SEM) and transmission electron microscopy (TEM). A correlation between the preparation conditions and optical and morphological characteristics of ZnS:Mn^{2+} powders was established.

Keywords: Zinc sulphide, Mn-doped nanoparticles, Photoluminescence

INTRODUCTION

Nanocrystalline materials have been of interest for more than 25 years [1-3]. The main cause is in their unusual properties based on the high concentration of atoms at interfacial structure and the relative simple ways of their preparation. Recently, nanoparticles of zinc sulphide have become the subject of intense investigations due to their potential applications in catalysis, sensors, nonlinear optics and molecular electronics [4-5]. At the same time, the synthesis of zinc sulphide (ZnS) particles with uniform morphology and narrow size distribution is still in the future and need to be further studied.

^a "Raluca Ripan" Institute for Research in Chemistry, "Babes-Bolyai" University, 30 Fântânele, RO-400294 Cluj-Napoca, Romania, cadisadi@chem.ubbcluj.ro

^b Faculty of Chemistry and Chemical Engineering, "Babes-Bolyai" University, 11 Arany Janos, RO-400028 Cluj-Napoca, Romania

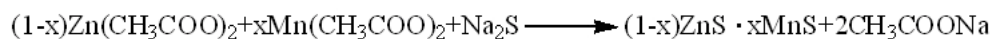
^c Electronic Microscopy Centre, "Babes-Bolyai" University, 5-7 Clinicilor, RO-400006 Cluj-Napoca, Romania

The increasing interest in these materials has lead to the development of a variety of chemical routes to prepare nanoparticles, including sputtering [6], ultrasound irradiation [7], co-evaporation [8], sol–gel method [9], solid-state reaction [10], gas-phase condensation [11], liquid-phase chemical precipitation [12], ion complex transformation [13], microwave irradiation [14] and biological synthesis [15]. From all these works, it has been found that particle size and luminescent properties of ZnS powders depend strongly on the specific preparation method and the applied experimental conditions.

This paper is the first in the series dedicated to the comparative investigation of luminescent and morphostructural properties of nanocrystalline ZnS:Mn powders obtained by different synthesis routes. In this respect, attempts to obtain manganese doped ZnS nanoparticles are performed by precipitation, using the sequential reagent addition technique (SeqAdd). In order to control the particle morphology and size, methacrylic acid is used as passivating agent. A systematic investigation on the influence of Mn-concentration on the photo-luminescence properties of nanocrystalline ZnS:Mn²⁺ is reported. A variety of methods including scanning electron microscopy (SEM), Fourier transform infrared spectroscopy (FTIR), and photoluminescence spectroscopy (PL) were used to characterise the ZnS:Mn nanoparticles.

RESULTS AND DISCUSSION

The goal of our study was to obtain luminescent manganese doped zinc sulphide ZnS:Mn²⁺ nanoparticles with controlled particle dimensions. In this purpose, attempts were made to prepare ZnS:Mn²⁺ powders, starting from Zn-Mn acetate mixture and sodium sulphide, in presence of methacrylic acid as particle size regulating agent. Precipitation was performed at low temperature, using SeqAdd technique. Zn-Mn acetate mixtures with variable compositions were used to obtain ZnS nanoparticles with variable Mn-doping level. The as obtained precipitation product can be considered as Zn-Mn double sulphide and the chemical process can be described by the overall equation:



In this manner, a series of 6 samples was prepared from mixture containing the following Mn/(Zn+Mn) ratios: 0 mol% (CAI17), 5.6 mol% (CAI19), 11.0 mol% (CAI73), 16.4 mol% (CAI21), 21.8 mol% (CAI20) and 25.0 mol% (CAI77). Mention has to be made that, the amount of incorporated Mn is about 0.1% of its concentration, as illustrated by the ICP measurements.

The as prepared ZnS powders show a high capacity to absorb anionic impurities from the precipitation medium, as exemplified by thermal analysis and FTIR spectroscopy.

The thermal behaviour of ZnS:Mn²⁺ powders was investigated in the 25-1100°C range, under N₂ flow. Thermogravimetric (TGA) and differential thermogravimetric (DTG) curves of ZnS powder are depicted in Figure 1. There are four major weight loss steps i.e. (1) - 7.2% at 20-188°C; (2) -9.9% at 188-300°C; (3) - 9.9 % at 300-850°C and (4) over 850°C that could be associated with: (1) removal of physically adsorbed water; (2) thermal dissociation of the acetate species adsorbed on the particle surface; (3) thermal dissociation and removal of organic compound and (4) sublimation of zinc sulphide, facilitated by the N₂ flow.

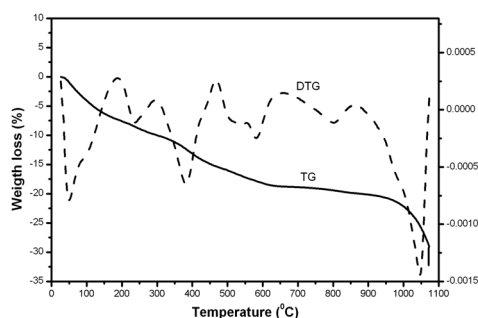


Figure 1. TGA and DTG curves for ZnS:Mn powder (CAI21)

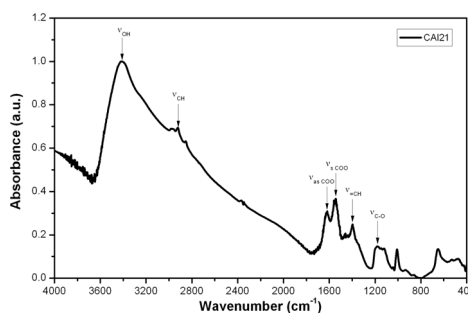


Figure 2. FT-IR spectrum of ZnS:Mn²⁺ sample (CAI21)

The FT-IR spectrum of ZnS:Mn²⁺ powder show the characteristic vibration bands for metal acetate, water and methacrylic acid, ionic or molecular compounds adsorbed from the precipitation medium (Fig.2.). The most important absorption bands are assigned as follows: hydroxyl groups (O-H) (between 3000 and 3600 cm⁻¹), CH₃ bending modes (950-1100 and 2800-3000 cm⁻¹), H₂O and COO group (between 1300 and 1600 cm⁻¹) and C=C and =CH groups (1000-1200 cm⁻¹) [16].

Mention has to be made of the large surface area of powders determines a high amount of anionic species to be adsorbed from the precipitation medium. In spite of the fact that all samples were carefully washed and centrifuged, the contaminants removal can not be completely done, due to the ZnS hydrolysis.

The as prepared manganese doped zinc sulphide powders show photoluminescence properties under ultraviolet excitation. Figure 3 shows the emission spectra ($\lambda_{exc} = 335$ nm) for samples synthesised from acetate

mixtures with different Mn^{2+} concentrations. Nanocrystalline ZnS:Mn^{2+} shows a weak blue emission (430 nm) and an orange emission (600 nm) under 335 nm excitation. The blue emission can be assigned to a defect-related emission of the ZnS host-lattice whereas the orange emission can be attributed to the ${}^4\text{T}_1\text{-}{}^6\text{A}_1$ transition of the Mn^{2+} ion.

The sample without Mn^{2+} shows only the ZnS-related blue emission. As soon as Mn^{2+} is incorporated in the ZnS nanoparticles, the intensity of the blue emission decreases and the Mn^{2+} emission comes up, since the energy transfer between ZnS host and Mn^{2+} impurity is very efficient. With an increasing Mn^{2+} concentration, the characteristic 600 nm emission becomes stronger.

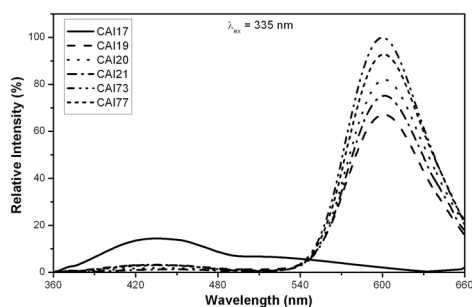


Figure 3. Emission spectra of ZnS:Mn^{2+} powders obtained from acetate mixtures with various Mn^{2+} concentration.

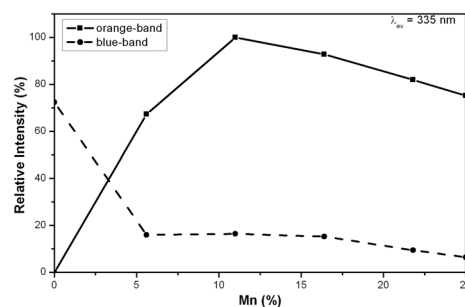


Figure 4. Relative intensity of the orange and blue bands *versus* Mn concentration (blue band is 5 times multiplied)

In figure 4, the luminescence intensity of the orange and blue bands is plotted as a function of the $\text{Mn}/(\text{Zn}+\text{Mn})$ ratio from acetate solution. The orange band intensity increases with Mn^{2+} concentration, in parallel with the increase of the emission centres numbers. At higher Mn-amounts, the luminescence intensity starts to decrease due to the mutual interaction between the doping (activator) ions (concentration quenching). The maximum intensity is reached at about 11% Mn^{2+} and corresponds to the optimum ratio between the number of the emission centres and the quenching ones. The blue band intensity decreases continuously with increasing Mn^{2+} amount, due to the decrease of the numbers of self activated centres related with the lattice defects of the zinc sulphide.

Usually the PL properties of ZnS powders are connected with a high temperature firing stage. In this case, the nanostructure state of ZnS powders determines the unexpected intense luminescence.

The morphology and particle dimensions were put in evidence by scanning (SEM) and transmission (TEM) electron microscopy investigations. The SEM image of CA121 sample shows that ZnS:Mn^{2+} powder consists of 1-3 μm aggregates of tightly packed particles with sizes under 20 nm (Fig. 5). The TEM image of the same sample illustrates that in fact, the ZnS:Mn^{2+} powder consists from very small particles (quantum dots) with diameters less than 3 nm. Due to the high surface area, these nanoparticles show a strong tendency toward agglomeration to much larger particles.

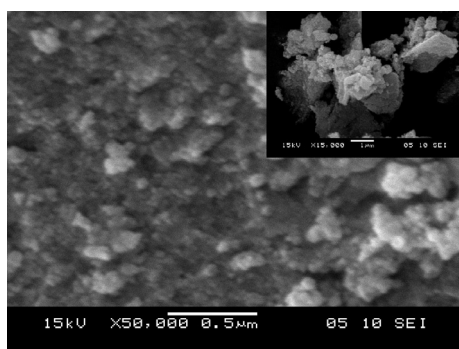


Figure 5. SEM image of ZnS:Mn^{2+} sample (inset scale bar = 1 μm)

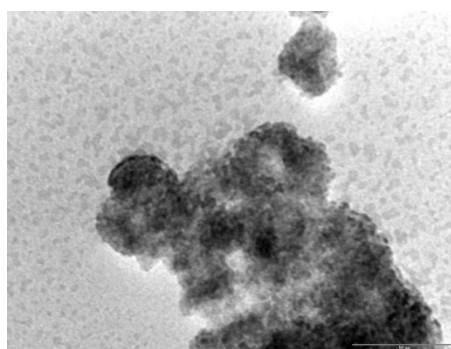


Figure 6. TEM image of ZnS:Mn^{2+} (scale bar=50 nm)

CONCLUSIONS

Manganese doped ZnS nanoparticles were obtained by precipitation, using the sequential reagent addition technique (SeqAdd). In order to control the particle morphology and size, methacrylic acid was used as particle regulating agent. The influence of Mn concentration on the luminescence properties of ZnS:Mn^{2+} nanocrystals was investigated. Photoluminescence measurements show that the as obtained ZnS:Mn nanopowders exhibit a strong orange emission centred at 600 nm that is related with the Mn emission centres. The maximum intensity is reached at about 11% Mn^{2+} in the Zn-Mn acetate mixture and corresponds to the optimum ratio between the number of the emission centres and the quenching ones. The strong PL of the un-annealed ZnS:Mn^{2+} powder could be associated with the particle nano-dimension.

Although ZnS:Mn^{2+} powders are formed from nano-sized crystallites (about 3 nm), they are tightly packed into larger and irregular shaped particles. The large surface area explains the high absorption capacity of the ZnS powder, as illustrated by TGA and FTIR investigations.

Supplementary work has to be done in order to improve the ZnS:Mn^{2+} powder dispersability.

EXPERIMENTAL SECTION

ZnS powders were prepared by precipitation, using SeqAdd technique, from Zn-Mn acetate and sodium sulphide in aqueous medium, at low temperatures (5°C). For this purpose, Zn-Mn acetate mixture containing 5.6, 11.0, 16.4, 21.8 and 25.0 mol Mn/100 mol (Zn+Mn) was prepared from 1M Zn(CH₃COO)₂ and 1M Mn(CH₃COO)₂ solutions and it was diluted with deionised water containing α -methacrylic acid (MA). The aqueous solution of Na₂S was added to the above mixture solution and vigorously stirred for 30 min. The resulting powder was washed and centrifuged, and finally dried at 80°C under vacuum. The wash process was performed with deionised water and isopropyl alcohol. As a comparison, pure ZnS nanoparticles were also prepared using the above method.

A METTLER-TOLEDO TGA/SDTA851 thermogravimeter was used for thermal and differential thermal gravimetry (TGA-DTG). The measurements were performed in alumina crucibles, in nitrogen flow (20 mL/min), with a heating rate of 5°C/min. Infrared absorption spectra (FTIR) of the samples prepared in KBr pellets were registered on a NICOLET 6700 FT-IR Spectrometer. Photoluminescence (PL) spectra were registered with JASCO FP-6500 Spectrofluorimeter Wavel equiped with photomultiplier PMT R928 (Farbglassfilter WG 320-ReichmannFeinoptik) and were normalized to the maximum intensity of the best sample (CAI73). The scanning electron microscopy (SEM) images were obtained with a JEOL-JSM 5510LV electron microscope using Au-coated powders. The accelerating voltage was 20 kV. The transmission electron microscopy (TEM) was performed with JEM JEOL 1010 microscope. The accelerating voltage was 20 kV.

ACKNOWLEDGMENTS

Financial support for this study was provided by the Romanian Ministry of Education, Research and Innovation (Project ID-2488).

REFERENCES

1. A. Henglein, *Berichte der Bunsengesellschaft für Physikalische Chemie*, **1982**, 86, 301.
2. H. Gleiter, *Progress in Materials Science*, **1989**, 33, 223.
3. L. F. Chen, Y. H. Shang, J. Xu, H. L. Liu, Y. Hu, *Journal of Dispersion Science and Technology*, **2006**, 27, 839.

4. J. Wen, G. L. Wilkes, *Chemistry of Materials*, **1996**, 8, 1667.
5. M. Miyake, T. Torimoto, M. Nishizawa, T. Sakata, H. Mori, H. Yoneyama, *Langmuir*, **1999**, 15, 2714.
6. S. K. Mandal, S. Chaudhuri, A. K. Pal, *Thin Solid Films*, **1992**, 350, 209.
7. A. R. Tomsa, E. J. Popovici, A. I. Cadis, M. Stefan, L. Barbu-Tudoran, S. Astilean, *Journal of Optoelectronics and Advanced Materials*, **2008**, 10, 2342.
8. R. Thielsch, T. Bohme, H. Bottcher, *Physica Status Solidi A*, **1996**, 155, 157.
9. B. Bhattacharjee, D. Ganguli, S. Chaudhuri, A. K. Pal, *Thin Solid Films*, **2002**, 422, 98.
10. P. Balaz, E. Boldizarova, E. Godocikova, J. Briancin, *Materials Letters*, **2003**, 57, 1585.
11. J. C. Sanchez-Lopez, A. Fernandez, *Thin Solid Films*, **1998**, 317, 497.
12. J. F. Suyver, S. F. Wuister, J. J. Kelly, A. Meijerink, *Nano Letters*, **2001**, 8, 429.
13. W. B. Sang, Y. B. Qian, J. H. Min, M. D. Li, L. L. Wang, W. M. Shi, Y. F. Liu, *Solid State Communications*, **2002**, 121, 475.
14. Y. Jiang, Y. J. Zhu, *Chemistry Letters*, **2004**, 33, 1390.
15. H. J. Bai, Z. M. Zhang, J. Gong, *Biotechnology Letters*, **2006**, 28, 1135.
16. N. B. Colthup, L. H. Daly, S. E. Wiberley, "Introduction to Infrared and Raman Spectroscopy", Academic Press, New York, **1964**.